J Mater Sci (2010) 45:2247–2257
DOI 10.1007/s10853-010-4236-7

REVIEW

Damage assessment in structural metallic materials for advanced nuclear plants

Wolfgang Hoffelner

Received: 8 November 2009 / Accepted: 12 January 2010 / Published online: 2 February 2010

Abstract Future advanced nuclear plants are considered to operate as cogeneration plants for electricity and heat. Metals and alloys will be the main portion of structural materials employed (including fuel claddings). Due to the operating conditions these materials are exposed to damaging conditions like creep, fatigue, irradiation and its combinations. The paper uses the most important alloys: ferritic-martensitic steels, superalloys, oxide dispersion strengthened steels and to some extent titanium aluminides to discuss its responses to these exposure conditions. Extrapolation of stress rupture data, creep strain, swelling, irradiation creep and creep–fatigue interactions are considered. Although the stress rupture- and the creep behavior seem to meet expectations, the long design lives of 60 years are really challenging for extrapolations and particularly questions like negligible creep or occurrence of diffusion creep need special attention. Ferritic matrices (including oxide dispersion strengthened (ODS), steels) have better irradiation swelling behavior than austenites. Presence and size of dispersoids having a strong influence on high-temperature strength bring only insignificant improvements in irradiation creep. A strain-range-separation based approach for creep–fatigue interactions is presented which allows a real prediction of creep–fatigue lives. An assessment of capabilities and limitations of advanced materials modeling tools with respect to damage development is given.

W. Hoffelner (✉)
Leader of "High Temperature Materials" Group,
Paul Scherrer Institute, Villigen,
Switzerland
e-mail: wolfgang.hoffelner@psi.ch; wolfgang.hoffelner@rwh.ch

Introduction

Carbon dioxide-free production of electric energy and alternative fuel are considered as cornerstones for future energy concepts [1]. These demands led to a worldwide recovery of interest in nuclear energy particularly for advanced nuclear power plants. Such plants should be able to operate with efficiencies significantly above the ones of current light water reactors, preferentially as combined cycle plants for co-generation of electric energy and heat. Such concepts were established within the international Generation IV initiative and published as a roadmap in 2002 [2]. From the six proposed plant types the sodium fast reactor (SFR) and the helium cooled high temperature reactor (HTR) are currently the most promising concepts for near-term deployment (typically 2020–2025). Particularly the HTR is intended to supply heat or steam for processes like synfuel or hydrogen production, refineries, chemical plants, metallurgical plants. In combination with other energy sources they are considered as a part of complex energy clusters [3, 4]. High temperature electrolysis (HTE), thermochemical cycles (e.g. iodine sulphur process) and steam reforming are currently under consideration as future options for hydrogen production with advanced nuclear power plants [3, 5]. These plants operate at high temperatures, in corroding environments and under irradiation. Such exposures cause materials damage of components during service. It is the aim of this paper to give an overview about damage occurring in the nuclear parts of such plants (including heat exchangers). Established metallic materials (e.g. ferritic-martensitic

steels) as well as advanced metallic materials are considered. Effects of corrosion are not included in this paper.

Materials

High-temperature stability and strength together with resistance against working environments (irradiation, atmosphere) and low costs are the main factors deciding on the materials used. The group of martensitic 9–12% Cr steels has a wide range of applications (pressure vessels, pipings, steam generators, advanced fission and fusion) for temperatures up to about 700 °C [6]. The martensitic structure cannot be used for higher temperatures. For temperatures above 700 °C nickel-base alloys or ferritic steels must be chosen. However, ferrites do not have the required creep strength and therefore they must be strengthened with additional obstacles for dislocation movement. Finely dispersed oxide particles in oxide dispersion strengthened (ODS) steels provide such a possibility. They also help to improve the creep strength of martensites which is the reason why martensitic ODS steels are intensely studied. ODS steels were produced on a commercial scale, e.g. by Plansee (PM2000) [7] or by Special Metals (MA956, MA957) [8].

Due to difficulties in component manufacture, welding and to the high prices, ODS materials did not manage a real breakthrough on the market. Lacking industrial demand led even to shut down of production facilities just recently. New activities with new grades of ODS are currently under development particularly for claddings of SFRs [9]. In this paper, examples from the classes of materials shown in Table 1 will be considered. During service the materials undergo different types of damage which are listed in Table 2. In this table, a discrimination is made between damage events on the micro-scale and on the macro-scale. The paper will be mainly concerned with creep, low-cycle fatigue, irradiation, creep–fatigue and irradiation creep.

Table 1 Conventional and advanced materials discussed in this paper

Type of material	Representative	Application
Ferritic-martensitic steels (without dispersoids)	Grade 91 steel	VHTR, GFR vessel, reactor internals, cladding
Ferritic-martensitic steels (with dispersoids or nano-precipitates)	PM2000, MA957, experimental grades of 9–12% Cr (martensites) and 12% < Cr < %20 (ferrites)	Cladding, structural parts (in-core, out of core)
Nickel-base superalloy	IN-617	Intermediate heat exchanger, piping, structural parts
Titanium aluminides	ABB-2 [10] γ/α_2-titanium-aluminide	Could replace superalloys in some applications. Included for assessment of potential

Table 2 Most important damage events encountered in plants of discussion

Exposure	Microscale	Macroscale
Temperature	Phase reactions, segregations	Hardening/softening, embrittlement
Irradiation	Displacement damage, phase reactions, segregations, helium damage	Hardening, embrittlement, swelling
Environment	Surface layer, local attack (pitting), grain boundary attack, formation of local stress raisers	Reduction of carrying cross section, subcritical crack growth, unexpected premature failure
Impact and static load	Dislocation movement, diffusion controlled dislocation and grain boundary processes	Plastic deformation, creep deformation, buckling, plastic collapse, sub-critical and critical crack growth, unexpected premature (catastrophic) failure
Cyclic load	Dislocation movement, local micro-crack formation, intrusions/extrusions	Cyclic softening, ratcheting, subcritical crack growth, premature failure
Combined exposures: Creep-fatigue, irradiation creep, corrosion fatigue, stress corrosion cracking	(Synergistic) damage accumulation	(Synergistic) damage accumulation, unexpected damage, premature failure

The discrimination between events on a microstructural scale and a macroscale refers to the different methods of analysis

Stress rupture and creep

Creep and stress rupture are very important properties for high-temperature applications. Improvements of the creep strength at temperatures up to about 700 °C are required for martensitic steels. Creep-resistant materials for temperatures up to 1000 °C are required for piping and heat exchangers for the very high temperature reactor (VHTR). Introduction of stable obstacles for dislocation movement is a well-known means to improve the stress rupture properties of alloys. Two routes are considered for advanced nuclear applications: precipitation of very fine M(C,N) precipitates or introduction of fine oxide dispersion into the matrix. As particle sizes are a few nanometers only, these steels are called "nano-structured" which does not mean that nano-grains exist. The development of MX-precipitation strengthening was strongly driven by ORNL [11–13]. The ODS materials which existed in commercial grades (previously introduced) were remarkably improved by Japanese researchers particularly with respect to SFR-cladding materials [9, 14]. Figure 1 shows a comparison of the stress–rupture properties of the most important established and advanced materials considered for advanced nuclear plants. As most of the ODS data in the literature were available as Larson Miller plots using 25 as constant all data were plotted with the same parameter. Two different applications were considered. Improvements of martensitic steels for temperatures up to roughly 650 °C with grade 91 as a reference and high-temperature applications with the nickel-base superalloy IN-617 as a reference. It can be seen that the ODS qualities are better than the non-ODS materials. However, the ODS data show considerable scatter. The TiAl-based alloy which was also included into this evaluation [15, 16] has about a factor of 2 (in stress) better stress rupture properties than IN-617. The thermo-mechanically treated (TMT) steel is better than grade 91. This is in agreement with other investigations on these steels where strength results together with first creep measurements let expect very good creep properties [12, 17].

Correlation of stress rupture data on the basis of LMP with a fixed constant is a very good tool to rank materials. One specific challenge for the applications under consideration is the fact that for key components life-times of 60 years and more are required which corresponds roughly with 500,000 h creep time. This provides some challenge for proper extrapolation, particularly when not sufficient long-term data exist. For this purpose, a LMP representation with a fixed value (without fitting the experimental values) would be not accurate enough. Some materials like e.g. grade 91, IN617 have been well investigated over the past and therefore a sound data set covering stress rupture data up to 100,000 h and more at least with a few points [18–20]. These data basically allow testing the predictive capabilities of different parameterizations like Larson-Miller [21], Manson Haferd [22], Minimum Commitment method [23] and others. An important question concerns the dependence of log t_R from temperature at constant stress (iso-stress curves). This is assumed to be either linear in T or linear in $1/T$.

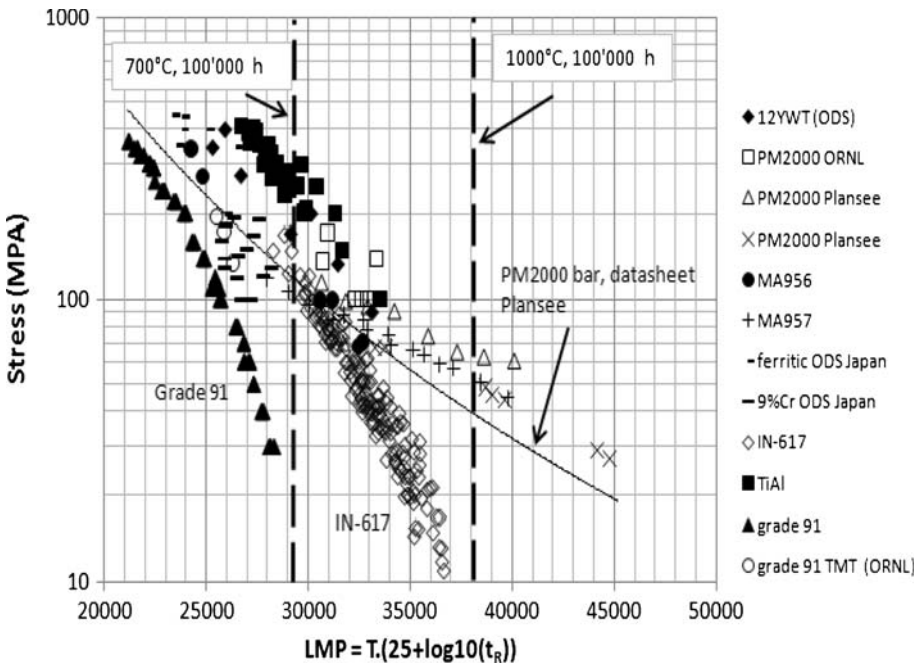

Fig. 1 Larson–Miller plot of several materials considered. Data from literature: 12YWT, PM2000, MA956, MA957 replotted from [25], ferritic ODS Japan, 1, 9% Cr ODS Japan replotted from [26, 88], IN617 replotted from [27], TiAl replotted from [15, 16], grade 91 replotted from [18], PM2000 bar parameterized according to Eq. 2 replotted from [28], grade 91TMT replotted from [12]. Two different applications were considered. Improvements of martensitic steels for temperatures up to roughly 650 °C with grade 91 as a reference and high-temperature applications with the nickel-base superalloy IN-617 as a reference

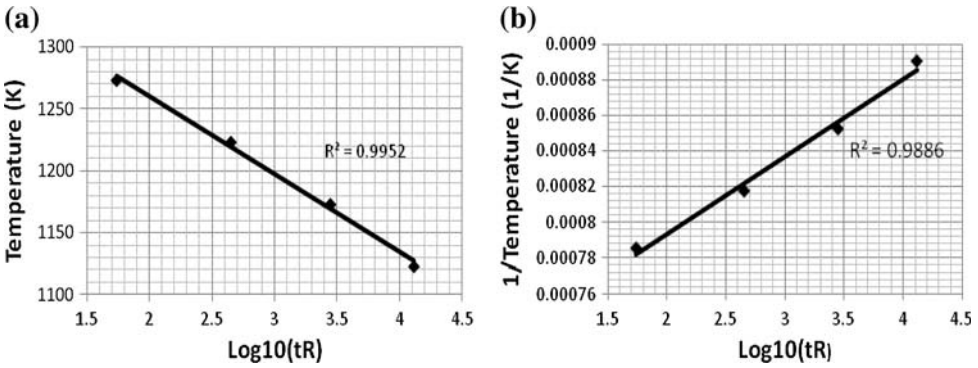

Fig. 2 Iso-stress plots of IN-617 at 40 MPa and correlation coefficient R^2. **a** $T - \log 10(t_R)$ plot; **b** $1/T - \log 10(t_R)$ plot. Data source: [27]

For e.g. the Larson-Miller approach as shown in Eq. 1, it is linear in $1/T$. Equation 2 is a parameterization using a T-dependence [24]. This method was used with very good success in former Brown Boveri Turbomachinery Development (today Alstom). Therefore, the respective parameter is abbreviated as C_{BBCP}.

$$\log 10(t_R) = (a \cdot (\log(\sigma))^3 + b \cdot (\log(\sigma))^2 + c \cdot \log 10(\sigma) + d)/T - C_{\mathrm{LMP}} \quad (1)$$

$$\log 10(t_R) = T \cdot (A \cdot \log 10(\sigma) + B \cdot \sigma + C) + C_{\mathrm{BBCP}} \quad (2)$$

where t_R is stress rupture time, σ is the applied stress, T is the temperature in K and a, b, c, d, C_{LMP}, A, B, C, C_{BBCP} are fitting parameters.

Basically, one would expect that one of the iso-stress plots correlates better with a linear function than the other. However, the interesting fact is that both plots show an equal linear behavior as shown in Fig. 2 for IN-617. The same behavior was also found for grade 91 steel. Performing the analysis for different stresses shows that the difference in correlation coefficient is not significant. This makes it understandable why the different parameterizations lead to equally good fits. Some care has to be taken for extrapolations over longer times where extrapolated stress rupture curves can eventually show quite unrealistic slopes [29]. The use of several parameterizations to determine the extrapolated values as a mean value between them all might be a possibility to come to more reliable extrapolations. This concept still needs further improvement.

Also, the effects of temperature or irradiation induced phase reactions occurring eventually after longer exposure times cannot be predicted this way. A link between the rupture time (t_R) and the steady state creep rate ($\dot{\varepsilon}$) is given by the Monkman–Grant rule. It is based on the experimental observation that the two quantities follow the simple relation given in Eq. 3:

$$t_R = A \cdot \dot{\varepsilon}^{\alpha} \quad (3)$$

with A and α being constants.

Figure 3 shows a Monkman–Grant plot of different materials: martensitic steels (12 Cr, T91 [30]), nickel-base

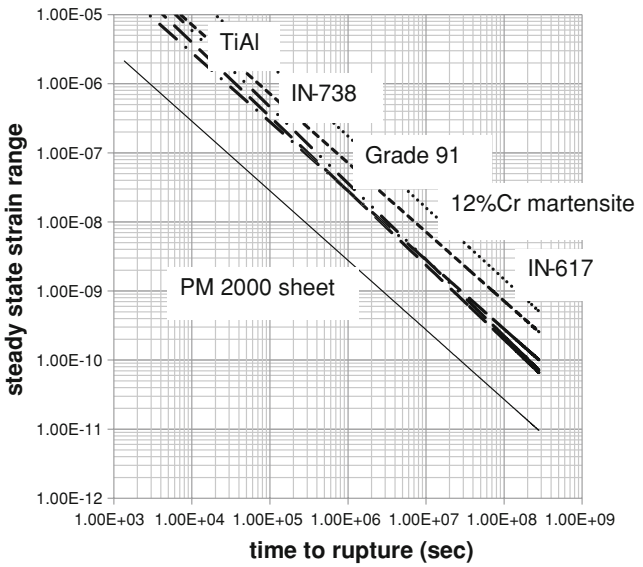

Fig. 3 Monkman–Grant plot of different material (average curves). Only the values for PM2000 seem to differ significantly

superalloys (IN617 [31], IN738) an intermetallic (TiAl) and a ferritic ODS alloy (PM2000). The curves agree surprisingly well. Only the ODS alloy seems to differ significantly from the other materials. Further tests are necessary to analyze this behavior more in detail. Similar to the Larson–Miller parameter with fixed constant also the Monkman–Grant rule is mainly a means to get first assessments of creep strain rates and to compare materials. In principle it had also the capability to serve as a basis for creep life assessments. Results gained with high creep rates at high stresses should also be representative for creep lives at lower stresses and longer times. However, such procedures should be done with necessary caution.

To illustrate that further a few other points should be mentioned which are currently studied with respect to advanced nuclear plants. The Monkman–Grant rule is based on the well-known Norton law which relates steady state creep rates and applied stress (Eq. 4). The Norton law is a technically very important constitutive equation.

$$\dot{\varepsilon} = A_2 \cdot \sigma^n \cdot \exp\left(-\frac{Q_a}{RT}\right) \quad (4)$$

Although it is a good description for a variety of materials, it is not necessarily always valid. Particularly for the superalloy IN617 conditions exist for which the Norton law is not valid as pointed out by Swindeman and Swindeman [32]. However, the experience of Schubert et al. [31] with the same material clearly shows a secondary (steady state) creep. This discrepancy is currently heavily discussed because of the importance of IN 617 and similar alloys for high-temperature applications like the intermediate heat exchanger in advanced nuclear plants. A basic understanding of this phenomenon is still missing. Another problem relates to the occurrence of diffusional creep for which a Norton exponent of 1 is expected. This could be confirmed for grade 91 material [33]. It can be expected that for long creep lives such effects have to be taken into consideration for component life-time assessments.

Eventual degradation of stress rupture properties during service by cyclic softening and/or thermally/irradiation induced microstructural changes is difficult to be predicted from short-term experiments with current damage assessment methods and improvements (e.g. advanced materials modeling as discussed in the last section) are required. The influence of cyclic softening will be treated in the fatigue section.

A final remark on creep and stress rupture concerns creep at lower temperatures. According to design codes an acceptable design should fulfill negligible creep criteria. Temperatures for reactor pressure vessels of VHTRs are expected to be between 320 °C (near-term deployment) and 420 °C (next generation). This requires consideration of long-term creep effects at low temperatures (cyclic softening, low-temperature creep). Recent investigations with fracture mechanics samples have shown that in this temperature regime pronounced creep effects can occur when the load is close to the yield strength [34]. Such questions and its consequences for safe design are currently under investigation as ASME-tasks [35].

Fatigue

Fatigue is usually divided into low cycle fatigue (high inelastic strain range) and high cycle fatigue (small to very small inelastic strain ranges). Low cycle fatigue (LCF) can be related to ductility. Materials with high ductility show normally higher LCF-lives than materials with low ductility. This can be understood as a result of ductility exhaustion which happens faster in materials with low ductility. The high cycle fatigue portion is governed mainly by the strength of the materials. This general behavior is also reflected in the fatigue curves of irradiated and oxide dispersion strengthened materials as shown in Fig. 4.

The data points were replotted from literature [36, 37]. The highest life-times for total strain ranges above 1% were found for the base materials (unirradiated and without dispersion). The dispersion leads to higher strength and lower ductility which is reflected in the fatigue curves. Irradiation to 30 dpa causes radiation hardening and radiation embrittlement. The loss of ductility lowers expectedly the fatigue lives below 1000 cycles. The irradiation hardening leads to a remarkable increase of the fatigue endurance in the high cycle regime.

The martensitic steel grade 91 shows very pronounced cyclic softening [38, 39] as shown as an example in Fig. 5.

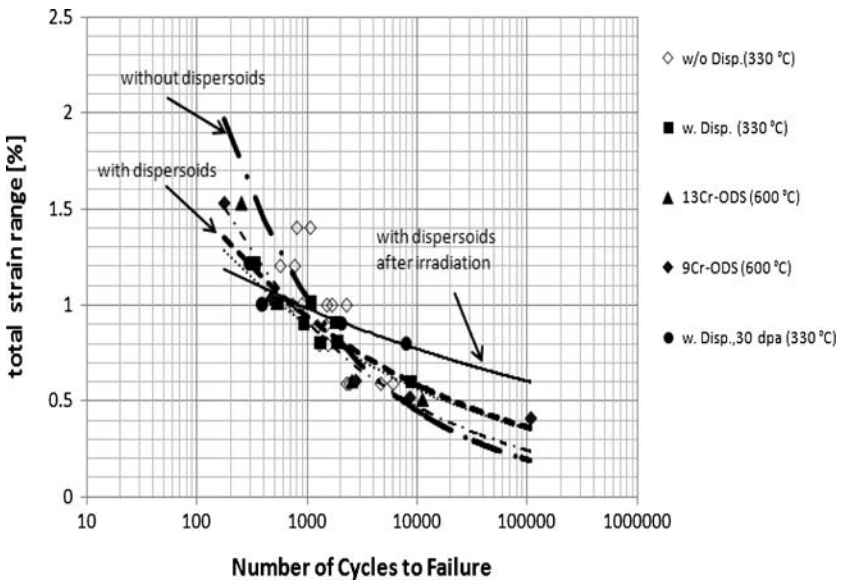

Fig. 4 Fatigue curves of a martensitic steel (EUROFER) in different conditions, with and without dispersoid [36]. Data for 13Cr-ODS and 9Cr-ODS [37] are also included. Although they were measured at higher temperatures, the fit into the general picture

This cyclic softening not only reduces the yield strength, it also increases the strain rates as a function of time to rupture (Monkman–Grant). For the determination of the correct strain rates, a reduced stress rupture curve could be derived [67] as shown in Fig. 6. Whether this curve represents the actual stress rupture curve of the material after cyclic softening or it can only serve as a means for determination of proper creep strain rates needs further experimental investigations. Basically, experimental evidence for a reduction of stress rupture lives as a result of cyclic softening exists [20, 89]. Other candidate materials do not show this strong cyclic softening behavior. This is particularly true for the martensitic ODS alloys as found by Ukai [36].

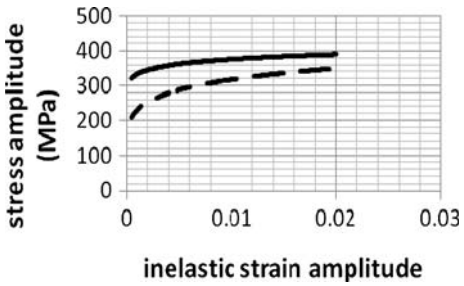

Fig. 5 Monotonic (*solid line*) and cyclic (*dashed line*) stress–strain curves at 550 °C for grade 91 material [39]

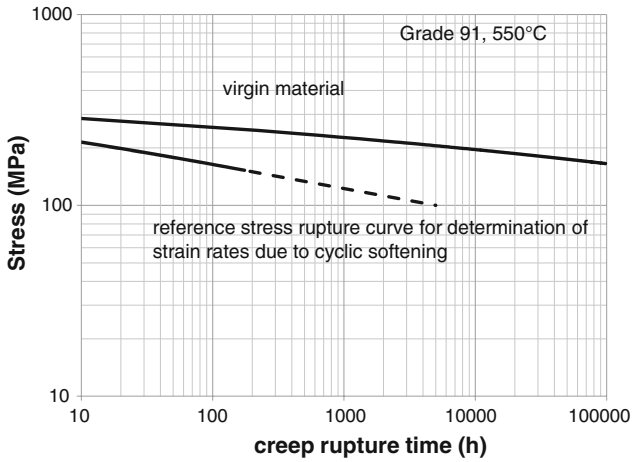

Fig. 6 Reference stress rupture curve for determination of creep rupture times from the Monkman–Grant rule to account for cyclic softening of grade 91 martensitic steel

Irradiation damage

Irradiation damage of steels has been extensively studied in the past (see e.g. [40–42]). The effects discussed in this paper concentrate mainly on topics which directly affect safety and life-time of components of advanced nuclear plants [43, 44]. Table 3 lists the following types of irradiation damage: displacement damage (formation of point defect clusters and loops), irradiation induced phase transformations and production of helium as a result of nuclear reactions. Results are swelling, irradiation hardening, and irradiation embrittlement. The very important effect of irradiation creep which happens when mechanical load and irradiation are simultaneously applied will be discussed in a separate section.

Swelling occurs as a result of point-defect agglomerations or voids which increase the volume. The need for operation at high temperatures would favor an austenitic matrix (iron- or nickel-base) possessing good creep resistance. Unfortunately, austenitic steels can show a pronounced swelling behavior [47]. Nickel is also very prone to radiation induced helium production and related materials degradation. The early US-experience with swelling of stainless steels is summarized in the following literature [45, 46]. Ferritic-martensitic steels show a much better swelling behaviour than austenitic steels (Fig. 7) [48, 49]. During the investigations on cladding materials for fast reactors it was found that oxide dispersion-strengthened versions of martensitic/ferritic steels had the potential to solve the high-temperature strength problem. They are also candidates for fuel cladding in future advanced reactors. Besides irradiation induced damage also helium-related damage can occur for fast spectra and particularly in fusion

Table 3 Modeling and model validation tools for analysis of component damage at different scales

Component damage	Modeling tools	Validation tools
Irradiation damage, phase diagrams and microstructural stability	Ab Initio, MD, thermodynamic modeling (kMC, rate theory)	Coordination chemistry, phases, magnetic issues (TEM, synchrotrons, neutrons, myons)
Mechanical properties (strength, toughness, etc.)	Dislocation dynamics (dislocation-obstacle interactions, dislocation patterning), MD	Micro(mechanical tests), dislocation arrangements, dislocation mechanisms (TEM)
Oxidation/corrosion	Ab initio, thermodynamic modeling, kMC	Chemistry, phase formation, (HR)TEM, EELS, beamlines
Fracture	Advanced FE, dislocation dynamics	Conventional samples

MD molecular dynamics, *kMC* kinetic Monte Carlo, *(HR)TEM* (high resolution) transmission electron microscope, *EELS* electron energy loss spectroscopy

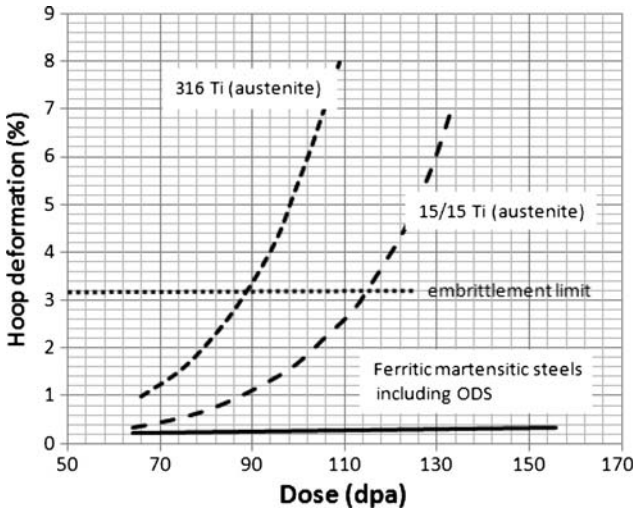

Fig. 7 Void swelling of two austenitic alloys compared with ferritic materials (including ferritic ODS). Data replotted from literature [48]

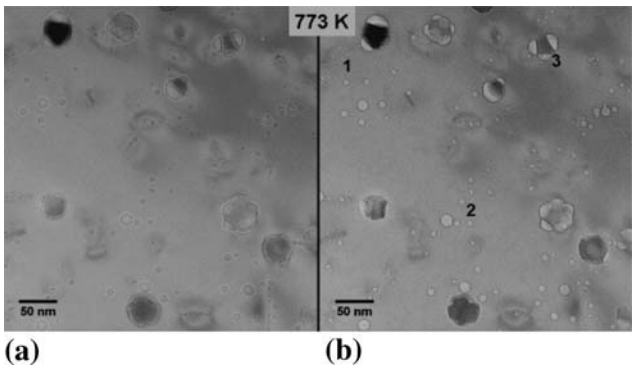

Fig. 8 Migration of helium to oxide dispersoids in the ferritic ODS alloy PM2000. Large bubbles are formed around dispersoids (3), intermediate size bubbles are either in the matrix or along dislocations (2), small bubbles are located at loops (1). Dislocations and loops are not visible under these contrast conditions. Replotted from Chen et al. [50]. **a** Over-focus; **b** under-focus

plants. Helium is a result of transmutant reactions. Helium diffuses to all kinds of sinks: point defects, dislocations and grain boundaries. Depending on its concentration it can form intragranular as well as intergranular clusters and bubbles. Helium bubbles at the grain boundaries considerably reduce toughness of a material. Helium is also attracted by dispersoids (Fig. 8) [50] which would be a key advantage of ODS steels in nuclear applications.

Very fine homogeneously distributed particles can act as sinks for helium preventing it from the formation of detrimental voids along the grain boundaries [51, 52]. This is one driving force behind current ODS developments of advanced ODS steels. For high temperatures, the ferritic-martensitic matrix is replaced by a high chromium ferritic matrix [53].

Creep under irradiation

The simultaneous presence of load, temperature and irradiation creates a combined damage process which leads to irreversible deformation of the material as a result of thermal creep, swelling and irradiation creep. Irradiation creep is an important type of damage for components operating in radiation environment at elevated temperatures. It can also become important for components operating at high temperatures during transients, when the temperature is still below the operating temperature and transient stresses become sufficiently high. Ferritic-martensitic materials (e.g. 2 1/4Cr–1Mo, HT9, 9Cr–1Mo) and austenitic materials (e.g. 304, 316, 321) and also nickel-base superalloys (e.g. PE19, IN-706, IN718) for claddings, low swelling blanket and bolting were important components studied. Many investigations were performed already about 30 years ago and they are well documented in the literature (see e.g. [54, 55]). In-reactor creep experiments with pressurized tubes of ferritic-martensitic steels were summarized in [56, 57]. Irradiation creep experiments are performed with pressurized tubes in reactors or with tensile, bending or torsion samples under ion implantation. High flux reactor experiments are usually performed to relatively high dose, whereas ion irradiation operates with high irradiation dose rates but to low total doses only. A summary of different types of irradiation creep experiments was given by Ryazanov [58] for austenitic steels. It was shown there that the irradiation creep compliance, C, remains constant for doses higher than 2 dpa and it almost linearly increases with decreasing dose below that value. In situations where swelling is insignificant, the irradiation creep compliance relates strain rate $\dot{\varepsilon}$, applied stress σ, and dose rate $\dot{dpa}$ according to Eq. 5.

$$C = \frac{\dot{\varepsilon}}{\sigma \cdot \dot{dpa}} \tag{5}$$

Most of the irradiation creep work with implantation was done below 2 dpa (experimental and financial restrictions), whereas the high flux neutron results were gained significantly above 2 dpa which could be an explanation why often higher irradiation creep rates were found under ion irradiation. Irradiation creep was studied with He-implantation for different qualities of ODS steels (average dispersoid diameters 25 and 2.2 nm). Also, the irradiation creep compliances of titanium aluminide were determined [59]. The results are plotted in Fig. 9 together with measurements on neutron irradiated creep samples from different ferritic and ferritic-martensitic steels [56, 57]. Several compliance values determined with He-implantation are in a relatively narrow scatterband. From these results no significant influence of the dispersoid size on irradiation creep is expected. Assuming a transient stage up

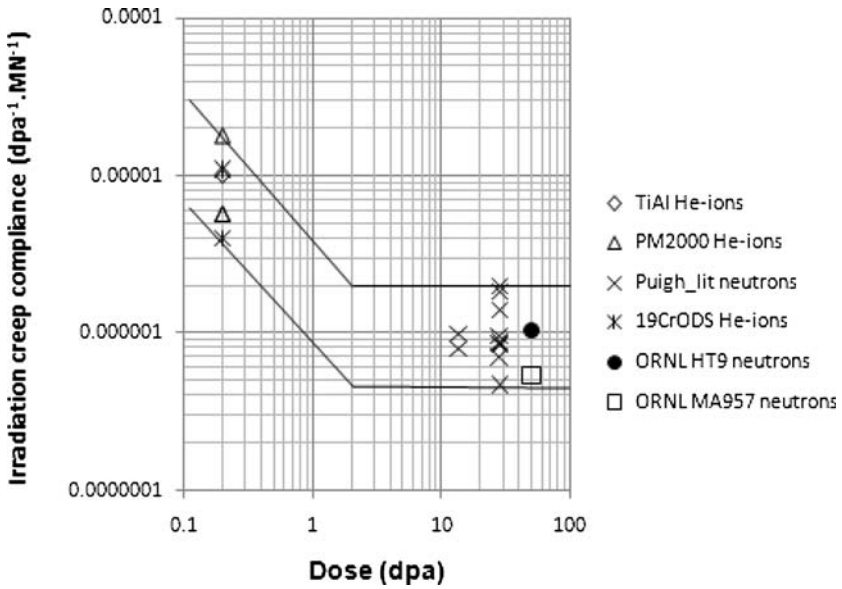

Fig. 9 Irradiation creep compliance for ferritic-martensitic steels in a temperature range from 300 to 600 °C [56, 57, 59, 60]. The two lines represent the scatterband of the data. The inflection points at 2 dpa were chosen based on a similar plot for austenitic steels [58]

to 2 dpa also a good agreement with conventional ferritic and ferritic-martensitic steels can be expected. Recent comparisons of the irradiation creep compliances of pressurized samples of HT9 (a ferritic martensitic material) with samples of MA957 (a ferritic martensitic ODS steel) under fast neutron irradiation revealed no significant differences between these two materials [60]. The average values of this investigation are plotted in Fig. 9 for comparison. They nicely fit the expectations. However, it should be mentioned that these average values can only be taken as a first assessment. Detailed findings reported in [60] (one point showing low compliance for MA957 at 300 °C and another showing high compliance of HT9 at 600 °C) still need further explanation. One possible explanation for enhanced irradiation creep at temperatures of about 600 °C could be that at this temperature thermal creep already becomes the important mechanism for this material. This behavior which was observed also for PM2000 and TiAl [61, 62] would explain also why no irradiation creep effects were detected for in-pile creep of advanced ODS materials at temperatures of 700 °C and higher [63]. These results seem to demonstrate that the presence of dispersoids does not have a significant influence on the irradiation creep behavior.

Creep–fatigue interactions

Another important type of damage interaction concerns creep and fatigue. Although attempts to get a sound understanding have lasted over the past 35 years, starting with the research published in the book "fatigue at elevated temperatures" [64], at least for design still the linear life fraction rule is used. It relates creep damage and fatigue damage in the following simple form:

$$\frac{t}{t_R} + \frac{N}{N_f} = D \tag{6}$$

where t is the creep time at certain stress, t_R stress rupture life at this stress, N number of cycles experienced at certain strain range, and N_f is the number of cycles to failure under this strain range. The damage D is sometimes set 1 or any other number (depending on the material). In design codes, like the ASME code, the limit line is usually given as a bi-linear plot which depends on the material (see Fig. 10). With the necessary modifications of existing design codes new attempts to find better representations of creep–fatigue interactions are currently under development [65]. These developments shall be illustrated taking the mod 9 Cr steel as an example. Due to the fact that this class of steels is used for fission-, fusion and non-nuclear applications, a huge database with creep–fatigue experiments exists which

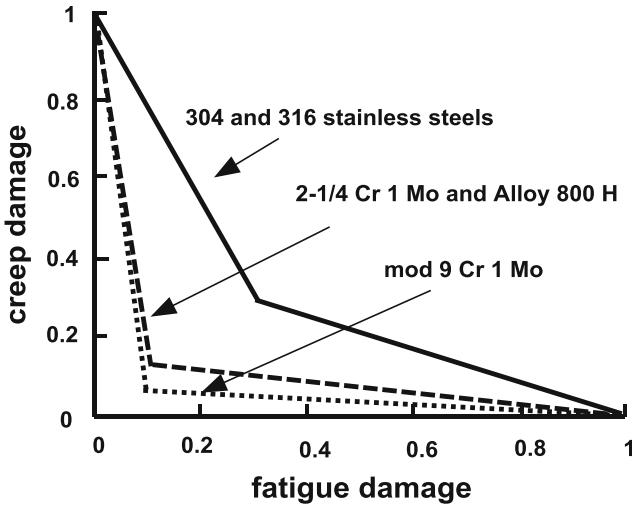

Fig. 10 Linear life fraction diagram for different materials according to the ASME code

is necessary to test different methods. Additionally, grade 91 steel shows substantial cyclic softening which is an additional challenge for life-time predictions. Many attempts were made in the literature to correlate creep–fatigue data for this material. Some of them are summarized in [66]. Often, they can correlate an existing set of creep–fatigue data, but they cannot make real predictions using different materials properties.

An approach which is based on a separation between plastic strain range and the pure creep strain range was recently proposed by the author [67]. It has its roots in Manson's strain range partitioning [68] which could be successfully employed to describe creep–fatigue interactions in gas turbine materials [69]. However, the method presented here considers only plastic strain range and creep strain range.

The whole procedure has been described in the literature [67] and therefore only the most important findings are summarized here. The Manson–Coffin lines for pure plastic deformation were determined from fatigue tests at high deformation rates which were taken from the literature [39]. Manson–Coffin lines for the pure cyclic creep portion were determined with the Monkman–Grant rule from reference stress–rupture curves after cyclic softening correction (see Fig. 6). The results of the evaluation are shown in Fig. 11. Only total strain ranges (0.4–1%), relaxation times (0.01–2 h tension, 0.05–1 h compression, up to 1 h/1 h in tension/compression) and creep time (up to 0.5 h tension, up to 0.2 h compression) were used as information to predict the life-times. All other information necessary to determine the number of cycles to failure was derived from stress–rupture curves, Monkman–Grant curve, S/N curves, static and cyclic stress–strain curves. The scatter of the data is a factor of 3 which is only slightly higher than the scatter of the pure fatigue data. This promising approach needs certainly to be further tested also with other materials,

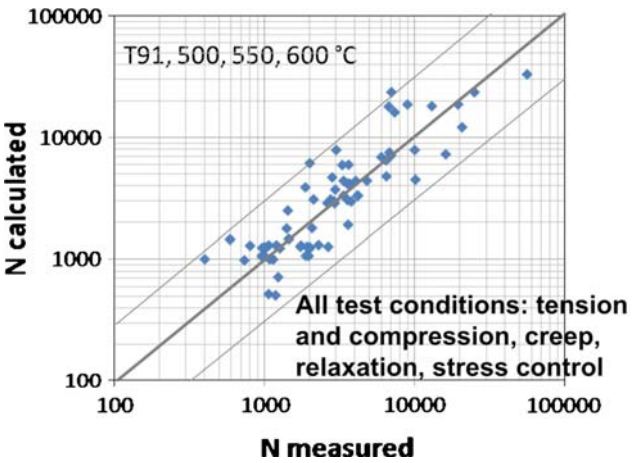

Fig. 11 Comparison of measured creep–fatigue lives with the ones determined with the strain range separation methods [67]. Material grade 91 steel

which will be done in the future once enough experimental creep fatigue tests exist.

Advanced methods for damage characterization

The demands to improve the accuracy of residual life assessments over long periods of time have led to the development of tools to model the materials behavior at different scales. Attempts to obtain information about materials properties relatively quickly without the necessity to have several long-term properties experimentally determined go into the same direction. Irradiation damage was one topic where modeling tools were used relatively early because the early stage of irradiation damage occurs on a time-scale which is well suited for atomistic modeling. Review papers on RPV embrittlement give examples of how atomistic modeling can be used [70, 71]. Atomistic modeling of irradiation embrittlement of RPV materials was also the main topic of the EU-PERFECT project [72] which was aimed at development of tools for modeling of irradiation damage in reactor pressure vessels. The current follow-up project PERFORM 60 [73] will enlarge these considerations to other reactor components. Irradiation damage is of particular interest for the fusion society. Based on the need to improve ferritic-martensitic steels for fusion applications, the atomistic behavior of the binary system Fe–Cr became particularly important [74]. A main portion of modeling related to fusion was done in the framework of the European EFDA-project (see e.g. [75]). Although these tools are still in its infancies (with respect to real-life damage), they have demonstrated its high potential for the future [76]. Modeling activities are also considered in the GENIV gas cooled reactor materials project [77, 78]. Phase stability, high-temperature strength and creep are most important for the VHTR, whereas irradiation induced damage is very important for gas cooled fast reactors. Table 3 summarizes different modeling and validation tools and how they could be used to contribute to the solution of technical challenges. Computational tools based on the CALPHAD (calculation of phase diagrams) approach are increasingly being used by industry to expedite alloy development [79]. The development of the nickelbase alloy 740 [80], a candidate for ultra supercritical superheater tubes for temperatures above 750 °C, is one very good example for the power of thermodynamic modeling. For modeling of microstructural properties of steels, the systems FeCr and FeCrC are investigated worldwide [81].

Dislocation dynamics together with MD simulations of dislocation-obstacle interactions seem to be able to predict particle strengthening quite well [82–85]. In this paper, it was only the aim to introduce materials modeling as a

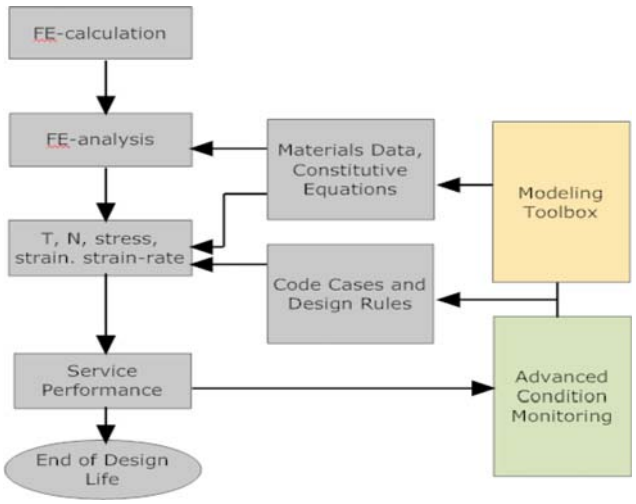

Fig. 12 Possible role of modeling and condition based monitoring for advanced damage assessment

possible future tool for better understanding of damage. However, a detailed discussion of materials modeling would go far beyond the scope of this article. Although the bulk of current modeling results were gained with model systems and for non-realistic operation conditions, it can be expected that these tools will help in future to improve the understanding of damage.

Combination of modeling with determination of local materials properties in terms of advanced micro- and nano-sample testing could become a powerful tool for damage assessments and residual life-time determination of plants in operation (Fig. 12) [86, 87]. Testing could be done on coupons or on material taken directly from the component. For micro-tests only very small amounts of sample material are necessary which means that the integrity of the component remains fully intact.

Acknowledgement The work presented was partially supported by the European Communities (EXTREMAT, RAPHAEL) and by ASME Llc./US DOE.

References

1. World Energy Outlook (2009) http://www.eia.doe.gov/oiaf/ieo/index.html
2. GENIV Roadmap. http://gif.inel.gov/roadmap
3. Next Generation Nuclear Plant. http://www.nextgenerationnuclearplant.com
4. Sustainable Nuclear Energy Technology Platform (SNETP). http://www.snetp.eu
5. HTTR Project Japan. http://httr.jaea.go.jp/eng/index_top_eng.html
6. Klueh RL, Harries DR (eds) (2001) High chromium ferritic and martensitic steels for nuclear applications. ASTM Bridgeport
7. Plansee PM2000, Technical Data Sheet. http://www.matweb.com/search/GetMatlsByTradename.aspx?navletter=P&tn=Plansee
8. Special Metals. http://www.specialmetals.com/products/index.php
9. Ukai S, Kaito T, Seki M, Mayorshin AA, Shishal OV (2005) J Nucl Sci Technol 42(1):109
10. Nazmy M, Staubli M. US Patent 5,207,982 and EP 45505 B1
11. Klueh RL, Hashimoto N, Maziasz PJ (2005) Development of new ferritic/martensitic steels for fusion applications, Fusion Engineering 2005, Twenty-first IEEE/NPS symposium (Sept 2005), pp 1–4. http://ieeexplore.ieee.org/stamp/stamp.jsp?arnumber=4018942&isnumber=401887
12. Klueh RL, Hashimoto N, Maziasz PJ (2007) J Nucl Mater 367–370(Part 1):1, 48–53
13. Klueh RL (2009) Trans Indian Inst Met 62(2):81
14. Kimura A, Cho Han-Sik, Toda N, Kasada R, Yutani K, Kisimoto H, Iwata N, Ukai S, Fujiwara M (2007) J Nucl Sci Technol 44(3):323
15. Lapin J, Nazmy M (2004) Mater Sci Eng A 380:298
16. Magnusson P, Chen J, Rebac T, Hoffelner W (2009) In: Shibli IA, Holdsworth SR (eds) Creep and fracture in high temperature components. DEStech Publ. Inc, pp 168–176
17. Klueh RL, Hashimoto N, Maziasz PJ (2005) Scr Mater 53(3):275
18. Cipolla L, Gabrel J (2005) New creep rupture assessment of grade 91. http://www.msm.cam.ac.uk/phasetrans/2005/LINK/162.pdf
19. Chandra S, Cotgrove R, Holdsworth SR, Schwienheer M, Spindler MW (2005) Creep rupture data assessments of alloy 617, ECCC conference, London
20. Tavassoli A-AF, Fournier B, Sauzay M (2009) Mater Res Soc Symp Proc, vol 1125. Materials Research Society, p 1125-R02-06
21. Larson FR, Miller EJ (1952) Trans ASME 74:765
22. Manson SS, Haferd AM (1953) A linear time-temperature relation for extrapolation of creep and stress rupture data, NACA TN 2890
23. Manson SS, Ensign CR (1979) ASME Trans J Eng Mater Technol 101:317
24. Hoffelner W (1986) In: Betz W et al (eds) High temperature alloys for gas turbines and other applications 1986. D. Reidel Publ. Comp., Dordrecht, p 413
25. Klueh RL, Shingledecker JP, Swindeman RW, Hoelzer DT (2005) J Nucl Mater 341(2–3):103
26. Ohtsuka S, Ukai S, Sakasegawa H, Fujiwara M, Kaito T, Narita T (2007) J Nucl Mater 367–370:160
27. Schubert F et al (1984) Nucl Technol 66:227
28. Hoffelner W, Chen J, Pouchon MA (2006) Thermal and irradiation creep of advanced high temperature materials, Proceedings HTR2006: 3rd international topical meeting on high temperature reactor technology, October 1–4, 2006, Johannesburg, South Africa, Conference proceeding paper E 00000038. http://www.nwu.ac.za/htr2006/static-content/downloads/final_download_papers/e/E00000038.pdf
29. Merckling G (2005) Long term creep rupture strength assessment: the development of the European Collaborative Creep Committee Post Assessment Tests, ECCC creep conference, 12–14 September 2005, London, pp 3–19
30. Swindeman RW, Mazlasz PJ, Brinkman CR (2002) Aging effects on the creep-rupture of 9Cr-IMo-V steel, Proceedings of 2000 international joint power generation conference, Miami Beach, FL, July 23–26, 2000
31. Schubert F, Penkalla HJ, Ullrich G. Creep-rupture behaviour, a criterion for the design of metallic HTR-components with high application temperatures. http://www.iaea.org/inisnkm/nkm/aws/htgr/fulltext/iwggcr4_24.pdf
32. Swindeman RW, Swindeman MJ (2008) Int J Press Vessels Piping 85:72
33. Gaffard V, Besson J, Gourgues-Lorenzon AF (2005) Int J Fracture 139
34. Wu R, Sandstrom R, Seitisleam F (2005) J Nucl Mater 336:279
35. Ramirez J (2007) McGreevy high temperature materials and design issues for Gen IV reactors, 19th international conference

on structural mechanics in reactor technology. http://www.engr.ncsu.edu/smirt-19/SMiRT19_WC3_McGreevy.pdf
36. Ukai S, Ohtsuka S (2007) J Nucl Mater 367–370:234
37. Petersen C, Povstyanko A, Prokhorov V, Fedoseev A, Makarov O, Walter M (2009) J Nucl Mater 386–388:299
38. Hirose T, Tanigawa H, Ando M, Kohyama A, Katoh Y, Narui M (2002) J Nucl Mater 307–311:304
39. LCF data T/P 91 NIMS database, last visit (2009)
40. Garner F, Hennager CH, Igata (eds) (1987) Influence of radiation on material properties, 13th international symposium (part II), ASTM STP956
41. Rosinski StT, Grossbeck ML, Allen TR, Kumar AS (eds) (2001) Effects of radiation on materials, 20th international symposium, ASTM STP1405
42. Stoller RE, Kumar AS, Gelles DS (eds) (1992) Effects of radiation on materials, 15th international symposium, ASTM STP ASTM
43. Allen T, St. Bruemmer, Elmer J, Kassner M, Motta A, Odette R, Stoller R, Was G, Wolfer W, St. Zinkle (2002) Higher temperature reactor materials workshop, Sponsored by the Department of Energy Office of Nuclear Energy, Science, and Technology (NE) and the Office of Basic Energy Sciences (BES), ANL-02/12
44. Rowcliffe AF, Mansur LK, Hoelzer DT, Nanstad RK (2009) J Nucl Mater 392:341
45. Porter DL. JOM 60(1) 20081047-4838 (print) 1543-1851 (online) issue
46. Allen TR, Busby JT, Klueh RL, Maloy SA, Toloczko MB (2008) JOM 60(1):15
47. Neustroev VS, Garner FA (2009) J Nucl Mater 386–388:157
48. Yvon P, Carré F (2009) J Nucl Mater 385:217
49. Klueh RL, Harries DR (eds) (2001) High-chromium ferritic and martensitic steels for nuclear applications, ASTM, pp 90–103
50. Chen J, Jung P, Hoffelner W, Ullmaier H (2008) Acta Mater 56(2):250
51. Yutani K, Kishimoto H, Kasada R, Kimura A (2007) J Nucl Mater 367–370:423
52. Odette GR, Miao P, Yamamoto T, Edwards DJ, Kurtz R, Tanagawa H (2008) A comparison of cavity formation in neutron irradiated nanostructured ferritic alloys and tempered martensitic steels at high He/dpa ratio, ORNL. http://www.ms.ornl.gov/programs/fusionmatls/pdf/June2008/3_FERRITIC/3.1_Odette_41-43.pdf
53. Kimura A, Cho HS, Toda N, Kasada R, Kishimoto H, Iwata N, Ukai S, Ohnuki S, Fujiwara M (2005) SuperODS Steels R&D, SMINS conference, Karlsruhe. http://www.nea.fr/html/science/struct_mater/Presentations/KIMURA.pdf
54. Garner FA, Perrin JS (eds) (1985) Effects of radiation on materials, Twelfth international symposium, ASTM Special Technical Publication 870, ASTM
55. Toloczko MB, Garner FA (2004) J ASTM Int 1(4). www.astm.org/JOURNALS/JAI/PAGES/JAI11372.htm
56. Puigh RJ (1985) In: Garner FA, Perrin JF (eds) Effects of radiation in materials. ASTM STP 870, ASTM, Philadelphia, pp 7–18
57. Gelles DS, Puigh RJ (1985) In: Garner FA, Perrin JF (eds) Effects of radiation on materials, Twelfth international symposium, ASTM STP 870, American Society for Testing and Materials, Philadelphia, pp 19–37
58. Ryazanov AI (2004) Modern problems of irradiation-induced plastic deformation in irradiated structural materials, Poster presented at Dislocations 2004, September 13–17, La Colle-sur-Loup, France
59. Magnusson P, Chen J, Hoffelner W (2009) Met Mater Trans A 40A:2837
60. Toloczko MB, Gelles DS, Garner FA, Kurtz RJ, Abe K (2004) J Nucl Mater 329–333:352
61. Chen J, Jung P, Nazmy M, Hoffelner W (2006) J Nucl Mater 352:36
62. Chen J, Hoffelner W (2009) J Nucl Mater 392(2):360
63. Kaito T, Ohtsuka S, Inoue M, Asayama T, Uwaba T, Mizuta S, Ukai S, Furukawa T, Ito C, Kagota E, Kitamura R, Aoyama T, Inoue T (2009) J Nucl Mater 386–388:294
64. Carden AE et al (eds) (1973) Fatigue at elevated temperatures, ASTM STP 520, ASTM
65. Hoffelner W (2007) Materials research for VHTR design codes, Structural materials for innovative nuclear systems (SMINS), Workshop proceedings, Karlsruhe, Germany, 4–6 June, pp 69–79
66. Christ H-J, Maier HJ, Teteruk R (2005) Trans Indian Inst Met 58(2–3):197
67. Hoffelner W (2009) Creep-fatigue life determination of grade 91 steel using a strain-range separation method, Proceedings of the 2009 ASME pressure vessel and piping conference PVP 2009, July 26–30, 2009, Prague, CZ, paper PVP2009-77705
68. Manson SS, Halford GR, Hirschberg MH (1971) Creep-fatigue analysis by SRP, Design for elevated temperature environment, ASME, pp 12–24
69. Hoffelner W, Melton KN, Wuethrich Ch (1983) Fat Eng Mater Struct 6(1):77
70. Odette GR, Lucas GE (2001) JOM 53(7):18
71. Soneda N (2008) In: Ghetta V, Gorse D, Mazière D, Pontikis V (eds) Materials issues for generation IV systems status, Open questions and challenges. Springer, Netherlands, pp 245–262
72. EU-Perfect project. https://fp6perfect.net/site/plaquetteD-10-09.pdf
73. Al Mazouzi A (2009) From perfect to perform. Accessed 13 May 2009. www.sckcen.be/en/content/download/5796/74801/file/RPV%201%20Almazouzi%20-%20The%20contribution%20of%20SCK%E2%80%A2CEN%20on%20reactor%20pressure%20vessel%20steels.pdf
74. Malerba L, Caro A, Wallenius J (2008) J Nucl Mater 382(2–3):112
75. Victoria M, Dudarev S, Boutard J, Diegele E, Lässer R, Mazouzi AAl, Caturla M, Fu C, Källne J, Malerba L, Nordlund K, Perlado M, Rieth M, Samaras M, Schäublin R, Singh B, Willaime F (2007) Fusion Eng Des 82:2413–2421 (ISSN 0920-3796)
76. Samaras M, Victoria M (2008) Mater Today 11(12):54
77. Samaras M, Hoffelner W, Chun Fu C, Guttmann M et al (2007) Revue Generale Nucleaire 5:50 (ISSN 0335-5004)
78. Samaras M, Hoffelner W, Victoria M (2007) J Nucl Mater 371:28 (ISSN 0022-3115)
79. Fahrmann MG, Smith GD (2002) JOM 54(1):42
80. Zhao SQ, Jiang Y, Dong JX, Xie XS (2006) Acta Metall Sin (Engl Lett) 19(6):425
81. Samaras M, Victoria M, Hoffelner W (2009) Nucl Eng Technol 41(1):1
82. Osetsky YN, Bacon DJ, Mohles V (2003) Philos Mag 83(31–34):3623
83. Takahashi A, Ghoniem NM (2008) J Mech Phys Solids 56:1534
84. Bako B, Weygand D, Samaras M, Chen J, Pouchon M, Gumbsch P, Hoffelner W (2007) Philos Mag A 87:3645
85. Bakó B, Weygand D, Samaras M, Hoffelner W, Zaiser M (2008) Phys Rev B 78:144104
86. Pouchon MA, Chen J, Ghisleni R, Michler J, Hoffelner W (2010) Exp Mech 50(1):79
87. Hoffelner W, Pouchon MA, Samaras M, Chen J, Froideval A (2008) Condition monitoring of high temperature components with sub-sized samples, Proceedings of the 4th international topical meeting on HTR technology, HTR 2008, September 28–October 1, Washington, DC, USA, HTR2008-58195
88. Sagaradse VV, Shalaev VI, Arbuzov VL, Goshchitskii BN, Tian Y, Qun W, Jiguang S (2001) J Nucl Mater 295:265
89. Binda L, Holdsworth SR, Mazza E (2009) In: Shibli IA, Holdsworth SR (eds) Creep and fracture in high temperature components. DEStech Publ. Inc